



1991 I. I. Rabi Award

Estimating Oxygen Saturation of Blood in Vivo with MR Imaging at 1.5 T¹

Graham A. Wright, MSc • Bob S. Hu, MD • Albert Macovski, PhD

The use of magnetic resonance (MR) imaging is investigated for noninvasively estimating the oxygen saturation of human blood (%HbO₂) in vivo by means of relaxation characteristics identified in earlier MR spectrometry studies. To this end, a sequence is presented for determining the T₂ of vascular blood in regions in which motions of the body and of the blood itself present a major challenge. With use of this sequence on a commercial 1.5-T whole-body imager, the relationship between the T₂ and %HbO₂ of blood is calibrated in vitro for the conditions expected in vivo. T₂ varies predictably from about 30 to 250 msec as %HbO₂ varies from 30% to 96%. T₂ values measured in situ for vascular blood in the mediastinum of several healthy subjects qualitatively reflected the behavior observed in vitro. Estimates of %HbO₂ for these vessels obtained with the in vitro calibration appear reasonable, particularly for venous blood, although difficulties arise in selecting the appropriate calibration factors. These encouraging initial results support a more systematic study of potential sources of error and an examination of the accuracy of in vivo measurements by comparison with direct measurements of %HbO₂ in vessels.

Index terms: Blood, MR studies, 94.1214 • Oxygen • Phantoms • Physics • Pulse sequences • Relaxometry

JMRI 1991; 1:275-283

Abbreviations: CPMG = Carr-Purcell-Meiboom-Gill, RF = radio frequency, S/N = signal-to-noise ratio, STIR = short inversion time inversion recovery, TI = inversion time, TR_e = effective recovery time, 2DFT = two-dimensional Fourier transform.

¹ From the Magnetic Resonance Systems Research Laboratory, 120 Durand, Stanford University, Stanford, CA 94305 (G.A.W., A.M.); and the Division of Cardiovascular Medicine, Stanford University Hospital, Stanford, Calif (B.S.H.). Received November 8, 1990; revision requested January 16, 1991; revision received and accepted February 11. Supported by the GE Medical Systems Group, the National Institutes of Health (contracts 1R01-HL-39478 and CA-50948) and the National Science Foundation (contract ECS-8801708). G.A.W. also supported by the Natural Sciences and Engineering Research Council of Canada. **Address reprint requests to G.A.W.**

© SMRI, 1991

THE DETERMINATION OF BLOOD OXYGEN saturation finds application in assessing cardiac output, consumption of oxygen in perfused organs, and the severity of vascular shunts such as those found in congenital heart diseases. Available oximetry methods are based primarily on optical transmittance and reflectance differences between oxy- and deoxyhemoglobin. The resulting measure of blood oxygen saturation is the percentage of hemoglobin that is oxygenated, abbreviated as %HbO₂. The poor penetration of tissue by light, however, limits the noninvasive monitoring of %HbO₂ to superficially accessible regions. The determination of oxygen saturation in deep vascular structures currently must be made via direct sampling of the blood of interest. In this report, we extend the current work relating the T₂ of blood (T_{2b}) in magnetic resonance (MR) studies to its oxygen saturation (1-3) for the purpose of noninvasively estimating %HbO₂ of vascular blood in vivo with a commercial whole-body imager.

Earlier investigators speculated that this goal should be attainable (1); however, to our knowledge, only qualitative in vivo signal variations attributed to the dependence of T_{2b} on %HbO₂ have been reported (4-6). Quantitative in vivo work demands a calibration of the T_{2b} versus %HbO₂ relationship for the specific experimental setup. The variations among experimental data fits for this relationship derived under a wide range of conditions with MR spectrometers (2,3,7,8) demonstrate that the underlying mechanism is not adequately understood. In particular, the parametric fit of the T_{2b} versus %HbO₂ relationship appears to be sensitive to field strength and the time between refocusing pulses in a way not predicted by the Luz-Meiboom model (9) used by most investigators (3). To our knowledge, only one study has directly measured T_{2b} for a wide range of %HbO₂. This study examined rat blood on a 4.3-T spectrometer that refocused the signal every 2 msec (2). Thus, for in vivo %HbO₂ estimation, this relationship must be experimentally quantified for conditions resembling

as closely as possible those to be used for human in vivo studies.

Before performing this calibration, we must address a more basic challenge: accurate estimation of $T2_b$ in vivo in a manner consistent with the estimation of %HbO₂. Difficulties that arise include (a) isolation of the blood signal of interest, (b) variation in signal strengths of blood at different TEs due to effects of flow such as wash-in of unexcited spins and dephasing, (c) artifacts due to motion (breathing and blood pulsatility), and (d) the poorer B₀ and B₁ homogeneity combined with weaker B₀ and B₁ fields available on whole-body imagers compared with those of spectrometers. This challenge is exacerbated because the vessels of interest include those of the mediastinum, where imaging conditions are the most demanding.

Here, we briefly review the available literature on the $T2_b$ versus %HbO₂ effect to derive a reasonable parametric model to fit to experimentally measured variations of $T2_b$ with %HbO₂ and to identify the basic structure for the in vivo sequence. From this foundation, we enhance the sequence to address the above practical issues. We then describe a series of experiments (a) to examine potential sources of bias in $T2$ measurements that might be introduced by the enhanced in vivo sequence or by the presence of flow, (b) to quantify the effect of %HbO₂ on $T2_b$ in vitro for the current setup, and (c) to measure $T2_b$ in vivo (particularly in the mediastinum) in healthy volunteers. Finally, with the in vitro calibration, we estimate the %HbO₂ of the in vivo blood from the $T2_b$ measurements and discuss factors affecting the accuracy and precision of such estimates.

● THEORY AND BACKGROUND

From work currently available in the literature, we identified the basic form of the relationship to be expected between $T2_b$ and %HbO₂ and the approximate sensitivity of $T2_b$ to %HbO₂ and to controllable sequence parameters. The latter is particularly useful for sequence design.

Functional Relationship between $T2_b$ and %HbO₂

The origin of the %HbO₂ effect on $T2_b$ is the irreversible dephasing of spins undergoing exchange and/or bounded diffusion through gradient fields in and around intact red blood cells. These gradients are established when B₀ is shifted for water inside the red blood cells due to the presence of paramagnetic deoxyhemoglobin. This frequency shift is proportional to the concentration of deoxyhemoglobin, found only therein (2,10), directly reflecting blood oxygen saturation. Rapidly and regularly applying 180° pulses reduces the range of frequencies a spin experiences before it is "refocused" and hence reduces the degree to which this loss of coherence is irreversible.

The Luz-Meiboom model of relaxation in the presence of exchange between two sites at different frequencies (9) is a good starting point for describing how this situation affects $T2_b$:

$$\frac{1}{T2_b} = \frac{1}{T2_o} + (P_A)(1 - P_A)\tau_{ex} \left[\left(1 - \frac{\%HbO_2}{100\%} \right) \alpha \omega_0 \right]^2 \times \left(1 - \frac{2\tau_{ex}}{\tau_{180}} \tanh \frac{\tau_{180}}{2\tau_{ex}} \right). \quad (1)$$

$T2_o$ is the $T2$ of fully oxygenated blood; τ_{ex} is a measure of the average time required for a proton to move between the two sites; ω_0 is the resonant proton frequency; α is a dimensionless value related to the susceptibility of deoxyhemoglobin and the geometry of the erythrocyte, so that $\alpha\omega_0[1 - (\%HbO_2/100\%)]$ can be considered the frequency difference between the two "sites" at which the protons exchange according to the Luz-Meiboom model; P_A is the fraction of protons resident at one of the sites under exchange; τ_{180} is the interval between refocusing 180° pulses in the MR imaging sequence. The strength of the %HbO₂ effect depends on field strength through the ω_0 term, increasing quadratically with B₀ and therefore favoring the use of high-field-strength imagers for the study. The sensitivity of $T2_b$ to %HbO₂ increases as τ_{180} increases, particularly when τ_{180} is on the order of τ_{ex} . Although the Luz-Meiboom model was developed with the assumption of many short refocusing pulses for which τ_{180} is much less than $T2$, simulations of the underlying exchange equations (11) indicate that the model is equally valid even when τ_{180} is equal to $T2_o$, as long as α remains relatively small (as it should in the current situation).

We do not require all the degrees of freedom given in the Luz-Meiboom model. We are interested in parameterizing the $T2_b$ versus %HbO₂ relationship in healthy subjects for a particular setup, not in exploring the details of the underlying mechanism as reflected by the parameters α , τ_{ex} , and P_A (3,8,12,13). These parameters can therefore be lumped into a single parameter K , which depends on the controllable variable τ_{180} . ω_0 is also subsumed under K for one field strength. Thus, measurements of $T2_b$ for a range of %HbO₂ will be fitted to a simplified Luz-Meiboom model for a small set of practical τ_{180} values:

$$\frac{1}{T2_b} = \frac{1}{T2_o} + K(\tau_{180}, \omega_0) \left(1 - \frac{\%HbO_2}{100\%} \right)^2. \quad (2)$$

Sensitivity of $T2_b$ to %HbO₂ and τ_{180} : Design Issues

Although we may not be able to establish from the literature the specific parameters relating %HbO₂ to $T2_b$, we can glean information about the order of magnitude of effects that will be valuable in designing our studies. The most basic issue is whether the %HbO₂ effect is great enough to be useful for our purposes. The size of the effect increases with operating field strength. Our studies are performed on a 1.5-T Signa unit (GE Medical Systems, Milwaukee). Apart from availability, it is well suited to this study because it is among the

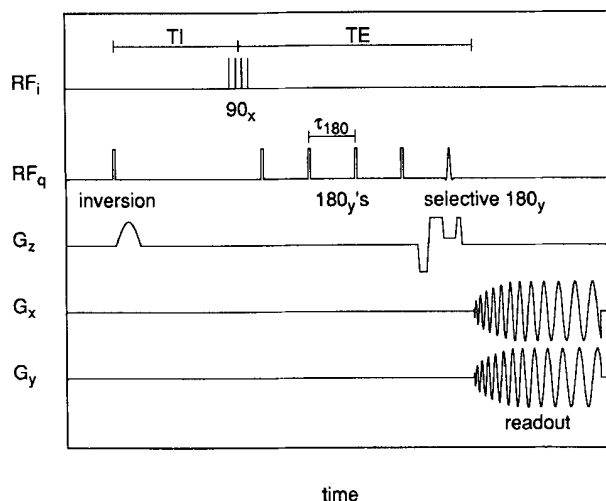


Figure 1. Pulse sequence for the in vivo estimation of T_{2b} . TI = inversion time. RF_i and RF_q are the in-phase and quadrature components of the RF field, respectively; G_x , G_y , and G_z are the field gradients applied along the corresponding spatial axes. As shown, the sequence images an axial section.

highest-field-strength whole-body imagers that are widely used.

In Equation (2), the size of the %HbO₂ effect is reflected in the parameters T_{2o} and K (for sufficiently large τ_{180}). When examining these parameters, we will consider only human blood under normal physiologic conditions—specifically, intact red blood cells suspended in plasma with a hematocrit around 45% and at 37°C. Temperature and hematocrit (7) affect T_{2o} and, to a lesser extent, K . Complete cell lysis eliminates the oxygen effect ($K = 0$), while the development of methemoglobin in intact cells found in clots will increase K (2,3). Under normal conditions, T_{2o} is approximately 220 msec \pm 30, per studies of oxygenated blood in a 1.4-T field (3,7). On the basis of the data fits of both Thulborn et al (2) and Bryant et al (7), $K(\tau_{180} \rightarrow \infty, B_0 = 1.5 \text{ T})$ is approximately 40 sec⁻¹. T_{2b} should be between 60 and 100 msec for sufficiently long τ_{180} when %HbO₂ is about 50%, the minimum level that is likely of interest for studies of vascular blood. This indicates that T_{2b} variations should be sufficient to reflect relatively small changes in %HbO₂.

A second question is how fast one can refocus the signal while still realizing most of the %HbO₂ effect (longer τ_{180} results in greater %HbO₂ effect). More rapid refocusing (shorter τ_{180}) is desirable to maintain spin coherence in the presence of complicated flow (14) and to provide a sufficient range of TEs to accurately estimate T_{2b} . The full Luz-Melboom model indicates that the dependence of $1/T_{2b}$ on τ_{180} is greatest for $\tau_{180} \approx \tau_{ex}$ and saturates as τ_{180} increases beyond about $5\tau_{ex}$. Ideally, we would use the value of τ_{180} at which this saturation begins. Independent of the above concerns, the minimum achievable τ_{180} is about 6 msec with the current experimental setup, limited by power absorption concerns and technical limitations of the radio-

frequency (RF) amplifier.

A reasonable τ_{180} is determined in part by the magnitude of the %HbO₂ effect. To accurately measure TE, τ_{180} should be at most on the order of half of the T_{2b} of interest. This suggests that we need only consider a τ_{180} of less than 50 msec. Where the saturation point for the effect of τ_{180} lies is not clear in the literature. Nonetheless, considering values of τ_{180} only up to 50 msec appears reasonable. From the data fits of Thulborn et al (determined primarily from data acquired at 4.3 T), one would not expect K to vary much with τ_{180} over the range of practical interest (>6 msec). From work performed primarily at 1.4 T (3,7), K should increase significantly as τ_{180} increases from 6 to 50 msec and should then level off slowly for further increases in τ_{180} .

● MATERIALS AND METHODS

As a foundation for the more detailed experimental descriptions, we first identify the complete in vivo sequence and its features and the relevant details of the imager platform used. Materials and methods specific to each of the three experiments proposed in the introduction (checking for bias in T_{2} estimation, calibrating T_{2b} dependence on %HbO₂ in vitro, and measuring T_{2b} in vivo) are then outlined. Since these experiments successively build on each other, it may be convenient for the reader to examine the results of each in the Results section before proceeding to the description of the subsequent experiment.

Sequence for Measurement of T_{2b} in Vivo

For spectrometer studies of blood, a CPMG (Carr-Purcell-Meiboom-Gill) sequence is used most often to measure T_{2b} . A version of this lies at the heart of the proposed sequence; however, we have made several modifications to address the challenges of the in vivo environment. The resulting sequence (Fig 1) is that originally introduced for the purpose of flow-independent angiography (14), augmented to include (a) spatial selectivity without wash-in effects, (b) reduced flow dephasing, and (c) faster image acquisition (to minimize, where necessary, effects of body motion).

To suppress fat signal, the sequence begins with a short TI inversion recovery (STIR) sequence ($TI = 120$ msec) followed by a frequency-selective 90° pulse that excites only the water protons (14). Fat is often found surrounding vessels and just under the skin. By eliminating its signal, one can minimize its contribution to signal measured in the vessel caused by partial-volume averaging and by blurring of fat signal (which occurs when one uses time-varying gradients of relatively long duration at data acquisition). Furthermore, artifacts from the normally high-signal-intensity fat in the chest wall that are due to breathing are suppressed. STIR minimizes the fat signal in the longitudinal magnetization at excitation, which has the added advantage of minimizing spurious signal from fat generated by the imperfect hard refocusing pulses that follow. Frequency-selective excitation provides additional fat suppression because it is difficult to

properly tune TI to achieve the desired level of suppression (14).

After excitation, the transverse magnetization is refocused every τ_{180} msec by rectangular 180° pulses. This pulse train establishes the constant refocusing interval required for accurate $T2_b$ estimation in the Luz-Meiboom model. It also restores the coherence of spins dephased because of flow through B_0 inhomogeneities (14). To minimize flow dephasing, spoiling gradients during the refocusing train are not used; however, this could lead to the propagation of spurious signals. One can generate strong spurious signals and lose significant amounts of desired signal because of errors in the axis and amplitude of flip angles, particularly when there are many pulses in the refocusing train. To minimize the effects of these errors, caused by B_0 and B_1 inhomogeneities, we vary the sign of the 180° pulses according to the MLEV pattern (15) whenever there are at least four pulses in the train (14). This pattern of sign variation is more robust than the standard CPMG pattern in the presence of B_0 inhomogeneities; however, under this scheme one should acquire signal only after 2^n pulses, where n is an integer.

As the first step in isolating blood signal by spatial location, the final refocusing 180° pulse is section selective and is bracketed by a pair of spoiling gradients to dephase the out-of-section signal. These gradients and the section-select gradient are flow compensated. Effects of wash-in and of the physical dispersion of tagged spins on blood signal are avoided because this is the only spatially selective pulse in the sequence and it is as close as possible to the data acquisition.

Finally, signal from the section is spatially encoded during data acquisition. We have implemented two variations of this. In the more standard case, we use the two-dimensional Fourier transform (2DFT) encoding of the original flow-independent angiography sequence (14). To minimize flow dephasing with this arrangement, all spatial-encoding gradients (notably the phase-encoding lobe and the dephasing lobe of the readout gradient) are kept compact and close to the data acquisition interval. In the second case, illustrated in Figure 1, spiral gradients rapidly cover k space during data acquisition (16). This version is useful when the duration of image acquisition is an issue. For instance, when imaging the chest, acquiring an entire image in a single breath hold minimizes motion effects. For this gain, we accept poorer signal-to-noise ratios (S/Ns) and greater sensitivity to blurring caused by B_0 inhomogeneity. Each spiral readout begins at the center of k space and at the center of the spin echo to minimize the effects of flow and B_0 inhomogeneities. Furthermore, the spiral trajectory has well-behaved gradient moments, maintaining flow coherence throughout the acquisition (16).

Timing of the data acquisitions can decrease sensitivity to the presence of flow. To prevent loss of coherence in subsequent echoes due to flow effects, signal is acquired at only one TE per excitation. To measure $T2$, we repeat the sequence at three to

four different TEs. To minimize effects of flow pulsatility, the sequence is gated to the cardiac cycle so that readout occurs in the same period of diastole independent of the selected TE. Data are acquired once every other heartbeat to maximize S/N per unit imaging time and to allow adequate $T1$ recovery to minimize effects of variable R-R intervals (14). Extra rectangular 180° pulses are included after acquisition for all but the longest TE of interest to ensure that the effective recovery time (TR_e) is independent of the TE at which the signal is received.

While the resulting sequence is rather involved, each element is chosen for its simplicity and/or availability with the objective of expeditious implementation. Potential variations include the use of crafted pulses for frequency-selective excitation or more robust refocusing (17,18), as well as alternative rapid acquisition strategies (19,20). These will be explored as the need arises from experimental work.

Imager Considerations

As noted earlier, all experiments were performed on a 1.5-T Signa unit. The system includes superconducting and resistive shims with which field variations of less than 20 Hz can be achieved over a 20-cm field of view in a uniform phantom. No supplementary shimming was done for individual experiments. Good shims minimize flow dephasing and diffusion effects during the refocusing train, as well as blurring when data are acquired with the spiral gradients. B_1 amplitudes are limited to about 625 Hz. The system is equipped with 10-mT/m gradients with which one can generate a 192×192 image of a 24-cm field of view in eight 40-msec spiral acquisitions (16). Shielded gradient coils minimize eddy current effects during such acquisitions. All cardiac gating was performed with a plethysmograph.

Experiment 1: Bias in $T2$ Measurement

Before experimenting on blood, we demonstrated that the features added to the sequence to address in vivo issues do not affect $T2$ estimation. We also showed that the sequence does not introduce measurement bias in the presence of flowing material. The phantom used in this study was plastic tubing with an inner diameter of 0.6 cm containing a manganese chloride solution with a $T1$ of approximately 1,200 msec and a $T2$ of approximately 120 msec. The tubing runs through a pump and settling system so that steady flow of fluid can be achieved. The phantom is a crude model of blood in a vessel. The tubing runs parallel to the main field in the magnet bore to minimize susceptibility effects. With the fluid stationary, we measured its $T2$ with the following sequences:

Sequence A: a standard multiecho 2DFT sequence with a TR of 2,000 msec and TEs of 48, 96, 144, and 192 msec (21), acquiring axial sections through the tube; $TR_e = 1,808$ msec.

Sequence B: a simplified version of the proposed sequence with only a rectangular excitation pulse, the train of hard refocusing pulses, each bracketed

Table 1
Estimates of T₂ of Phantom under Various
Experimental Conditions

Sequence	τ_{180} (msec)	Flow Rate (cm/sec)	T ₂ (msec)
A	48	0	95
B	48	0	121
B	24	0	122
C	24	0	121
C	24	9	116
C	24	18	117
C	24	28	115
C	12	18	115
C	6	18	120

Note.—See text for explanation of sequences.

by spoiling gradients, and a 2DFT phase encoding and readout to produce coronal projection images (14). One TE is acquired per excitation; $\tau_{180} = 24$ msec; TE = 48, 96, and 192 msec; TR_e = 1,808 msec for each image. This sequence is also repeated with a τ_{180} of 24 msec; TEs of 24, 48, 96, 192, and 384 msec; and a TR_e of 2,000 msec.

Sequence C: the complete proposed sequence, including STIR, frequency-selective excitation, the refocusing train without spoiling gradients, a final spatially selective pulse, and spiral gradients during data acquisition to generate axial sections. $\tau_{180} = 24$ msec; TE = 24, 72, 120, 216, and 408 msec; TR = 2,000 msec. Extra refocusing pulses after data acquisition make the effective T₁ recovery time, TR_e, 1,592 msec for each TE.

The effects of flow on T_{2b} measurement were examined with sequence C in the presence of steady flows of 9, 18, and 30 cm/sec. For a flow of 18 cm/sec, this sequence was repeated with τ_{180} values of 6 and 12 msec to ensure that varying the refocusing rate in the presence of flow does not bias T_{2b} measurements.

In these and all later experiments, T₂ values were estimated with a weighted least-squares fit of a monoexponential decay to the average signal intensities in a small region of the phantom (21,22).

Experiment 2: In Vitro Calibration of T_{2b} versus %HbO₂

To establish a quantitative relationship between T_{2b} and %HbO₂, the T_{2s} of human blood oxygenated to varying degrees were measured for a practical range of τ_{180} values. The parameters *K* and T_{2o} of Equation (2) were determined by a least-squares fit to the resulting data.

Blood was drawn via venipuncture from five healthy volunteers after their informed consent was obtained. In some cases, the subject's arm was cooled in water (18°C) to reduce oxygen saturation of the venous blood. No chemicals were added to further reduce %HbO₂. The samples were citrated and then aerated to varying levels of %HbO₂ (as measured with a reflectance oximeter [American Optical, Buffalo]), starting at the level at which the blood was drawn. The samples were then stored in evacuated 5-mL glass tubes in which the %HbO₂ levels could be maintained for several hours. This was confirmed by remeasuring the %HbO₂ of each

sample after the T_{2b} measurements. Hematocrit was also measured at this time.

Data for the T_{2b} measurements were acquired within 2 hours after the original blood drawing. Before imaging, sets of blood-containing tubes were immersed in an insulated bath of water doped with MnCl₂ (T₂ < 2 msec) at 37°C to minimize B₀ inhomogeneity due to susceptibility and to maintain the blood at body temperature throughout the experiment. A head coil was used for excitation and signal reception. For greater S/N and reduced susceptibility effects, sequence B, the simplified version described in the previous section, was used to measure the T_{2b} values. Specifically, T_{2b} values were measured for τ_{180} values of 6, 12, 24, and 48 msec. For each τ_{180} , signals were acquired at TEs ranging from 24 to 384 msec; TR_e was 2,000 msec. Before each set of measurements, the samples were agitated to minimize settling effects. Sequence C was also run in a subset of the experiments to check for any differences when imaging blood.

Experiment 3: In Vivo Studies

Using the complete in vivo sequence (sequence C), we measured T_{2b} in several vessels of clinical interest—primarily the aorta, superior vena cava, and pulmonary trunk—in several healthy volunteers (with their informed consent). The signals from these vessels were isolated by acquiring an axial section through the pulmonary trunk while the subject lay prone, with a circular surface coil 18 cm in diameter beneath the chest to receive the signal. With use of spiral gradients during readout and reception of signal every other heartbeat during diastole, an image could be acquired in 16 heartbeats, during which the subjects held their breath. This breath-hold interval is quite reasonable for the current study of healthy subjects; however, further development may be required to reduce this interval in patient studies. The resulting image has a resolution of 1.7 × 1.7 × 10 mm. To estimate T_{2b}, we acquired four to five images at TEs ranging from 24 to 408 msec. For most subjects, the signal was refocused every 24 msec (deemed best from the in vitro calibration; see Results). We repeated the studies using τ_{180} values of 6 and 12 msec in three subjects to demonstrate the effect of τ_{180} in vivo. T_{2b} values were also estimated with 2DFT data acquisition for vessels in an axial section of the arm and for the descending aorta and inferior vena cava in an axial section of the abdomen in individual subjects.

● RESULTS AND DISCUSSION

Experiment 1: Bias in T₂ Measurement

T₂ estimates for the phantom, obtained with the various sequences, are listed in Table 1. In all cases, monoexponential decay fit the data well. The standard error in repeat measurements of T₂ was about 3 msec. The commercial multiecho sequence (A) yielded significantly smaller T₂ estimates than the two versions (B and C) of the proposed sequence. When we repeated the measurements with the commercial sequence but used only a single

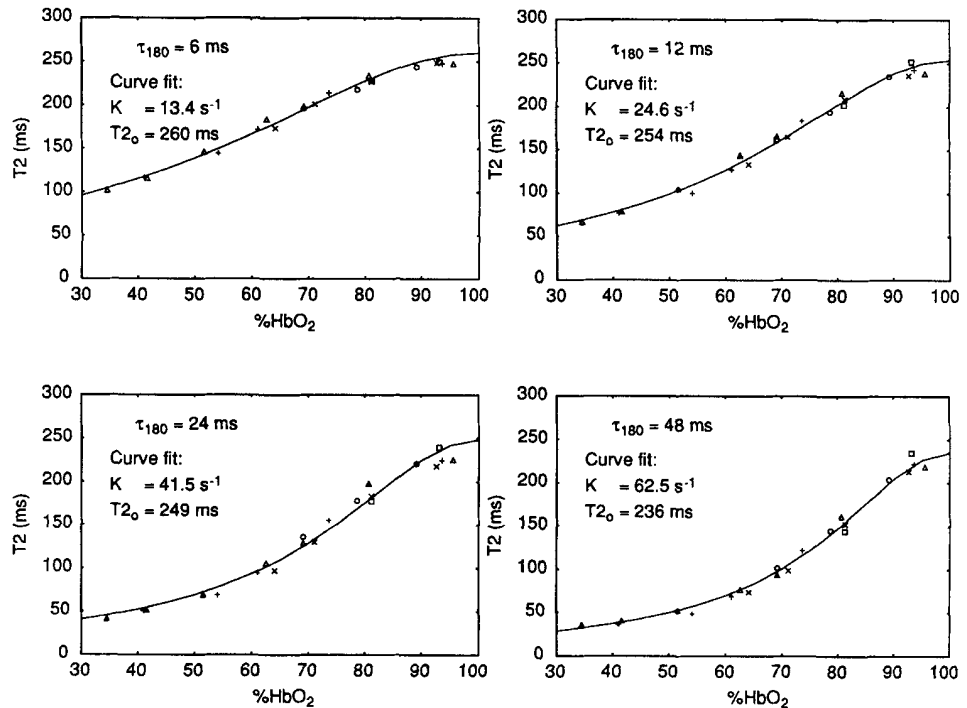


Figure 3. $T2_b$ versus %HbO₂ data fits. Each graph corresponds to a different τ_{180} (as indicated). Different point symbols refer to different subjects. Solid line is the least-squares fit of Equation (2) to the data; corresponding estimates of K and $T2_0$ are indicated.

echo per acquisition and a very long TR, we obtained $T2$ values comparable with those found with sequences B and C. Hence, the commercial multi-echo sequence appears to introduce a biasing error. Further investigation of this problem was beyond the scope of this study; however, potential sources of such errors in multi-echo sequences on imagers have been investigated by others (23,24). Both the simplified version (B) and the complete version (C) of the proposed sequence yielded the same $T2$ values for stationary fluid. $T2$ measurements with sequence C were relatively independent of velocity for steady flows. Similarly, varying τ_{180} in the presence of steady flow did not affect $T2$ measurements. Thus, the proposed sequence seems to reflect true transverse relaxation under various conditions. These results also add credence to the use of the relationship between $T2_b$ and %HbO₂—established with in vitro experiments in which stationary blood was imaged with sequence B—in estimating %HbO₂ levels of flowing blood in vivo from $T2_b$ determined with sequence C.

Experiment 2: In Vitro Calibration of $T2_b$ versus %HbO₂

The blood samples used in this experiment had %HbO₂ levels ranging from 30% to 96%. Direct %HbO₂ measurements in the samples, obtained before and after $T2_b$ measurements, differed on average by about 2%. Hematocrits in different subjects ranged from 42% to 47%. The integrity of the erythrocytes was maintained throughout the study, on the basis of examination of centrifuged samples.

Figure 2 depicts one of the images used for the estimation of $T2_b$. The variation in intensity with oxygen saturation of the blood is readily apparent on

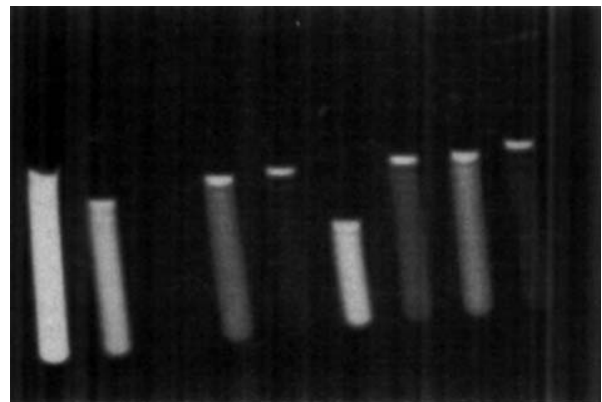


Figure 2. Projection image ($\tau_{180} = 24$ msec, TE = 96 msec) of blood samples from one subject. Test tube at far left contains doped water. Remaining tubes contain blood with varying %HbO₂: from left, 80, 62, 35, 95, 52, 69, and 42.

this $T2$ -weighted image. The $T2_b$ of each sample was estimated from the average signal intensity determined in a small square region at about the center of the sample.

Transverse relaxation of the blood is well described by monoexponential decay. Most errors in fitting this model to the measured signal intensities can be attributed to random noise in the raw data, on the basis of the results of χ^2 tests (21). The resulting estimates of $T2_b$ are plotted in Figure 3 as a function of the %HbO₂ measured for the corresponding samples. Standard errors in the estimates of $T2_b$, based on propagation of random noise in the raw images (25), range from approximately 0.5

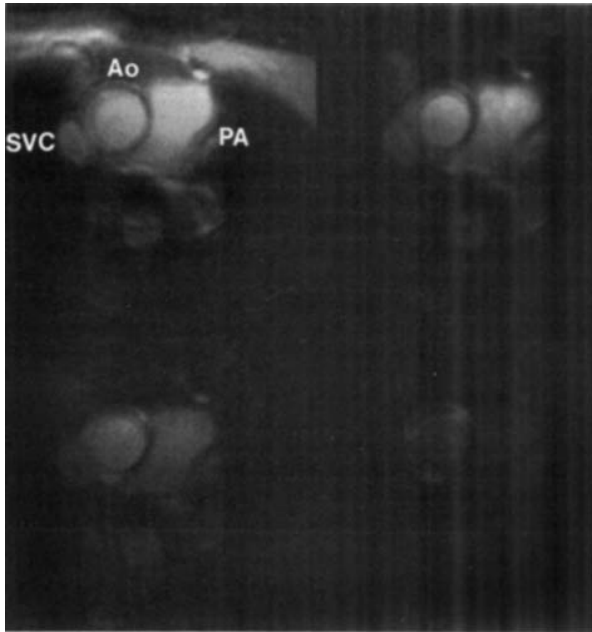


Figure 4. Images used for the estimation of $T2_b$ in vivo. Axial section through the pulmonary trunk is shown at various TEs (clockwise from upper left, 24, 120, 408, and 216 msec). SVC = superior vena cava, Ao = ascending aorta, PA = pulmonary artery.

msec for a $T2_b$ of 30 msec to 5 msec for a $T2_b$ of 250 msec. For each τ_{180} , we estimated K and $T2_o$ via a least-squares fit of Equation (2) to the data, weighted to allow for the expected error in the $T2_b$ values. The resulting parametric values and the corresponding curve fits are presented in Figure 3.

Equation (2) provides a reasonable fit to the data. There is strong evidence that K varies with τ_{180} over the range studied (6–48 msec), in general concurrence with spectrometry studies at about the same field strength (3,7); however, our limited data would yield somewhat lower estimates of τ_{ex} (3–5 msec). As discussed in the Theory and Background section, the minimum τ_{180} value for which K is close to its maximum should be used. The larger K reflects a greater $\%HbO_2$ effect, minimizing the propagation of error from the $T2_b$ measurement to the $\%HbO_2$ estimate. Earlier work, as well as current results, indicates that the influence of τ_{180} on K decreases as τ_{180} increases beyond approximately 24 msec, although we still see a significant change from 24 to 48 msec. Using a τ_{180} of 24 msec gives a reasonable trade-off between maximizing K and minimizing flow effects and provides a sufficient range of TEs for estimating $T2_b$.

Under this arrangement, the standard error in predicting $\%HbO_2$ from $T2_b$ measured in vitro is about 2.5% over the range of clinical interest ($\%HbO_2 < 90\%$). The reflectance oximeter used as our "gold standard" is accurate to $\pm 2\%$ in this range, so this reference is potentially a major source of error. For clinical work, accuracy to within 3% is generally acceptable. For the $\%HbO_2$ range of arterial blood ($>90\%$), the model suggests

that $T2_b$ is much less sensitive to $\%HbO_2$ in general, predicting poorer accuracy for such estimates. This may not be a major concern in clinical work because one often simply assumes that arterial blood is fully oxygenated or one uses values of arterial $\%HbO_2$ measured in surface regions with a pulse oximeter. Hence, the current level of accuracy of $\%HbO_2$ estimates would be practically useful if it could be achieved in vivo.

These initial results justified preliminary in vivo studies in healthy volunteers. However, several areas for further development in these calibration studies are in order. For this report, studies were limited to healthy individuals with a narrow range of normal blood characteristics. The effects of variations in blood characteristics among different individuals on the calibration and the accuracy of Equation (2) as a model of the relation between $T2_b$ and $\%HbO_2$ are both areas of interest in expanded studies. As noted in the Theory and Background section, these are subjects of increasing scrutiny in the research community, yielding a growing body of applicable literature.

Of particular interest is the effect of individual differences in hematocrit. There is evidence that $1/T2_o$ varies linearly with hematocrit (7) while K varies quadratically (2). On the basis of these results, for hematocrits ranging from 30% to 50% (an extreme range encompassing many pathologic conditions), changes in K would introduce at most a 3% error in $\%HbO_2$ if not accounted for, while changes in $T2_o$ would yield substantially greater errors. In our work, estimates of K for a given τ_{180} were consistent from subject to subject, while there was weak evidence of individual differences in the parameter $T2_o$ (although these differences did not appear to correlate with the small variations in hematocrit). We will extend our calibration studies in future work to span physiologic or pathologic variations in erythrocyte density (ie, hematocrit) and variations in properties such as erythrocyte size and shape, to determine the need for calibration corrections for particular patients. If such corrections are necessary, they could be realized in a clinical situation by measuring the relevant properties of a patient's blood obtained via venipuncture.

Our current results also raise questions regarding the accuracy of the model. $T2_o$ tends to decrease slightly with increasing τ_{180} , although the theory supporting the model suggests that $T2_o$ should be independent of τ_{180} . No effect of τ_{180} on the T2 of doped water, used as a control in the experiments, was observed; hence, the effect seems to be specific to blood and not easily explained as a reduced diffusion effect. The results of Gomori et al (3) in the measurement of the T2 of fully oxygenated blood for various τ_{180} values reflect this effect, although the authors do not discuss the anomaly. Clearly, further study of $T2_o$ would be of merit, with respect to individual differences and to the accuracy of the model.

Experiment 3: In Vivo Studies

Figure 4 shows a set of images of an axial section through the pulmonary trunk in one volunteer, ac-

Table 2
%HbO₂ Estimates from Measurements of T_{2b} in Vivo

Subject	T _{2o} (msec)*	τ ₁₈₀ (msec)	Aorta		Superior Vena Cava		Pulmonary Trunk	
			T _{2b} (msec)	%HbO ₂	T _{2b} (msec)	%HbO ₂	T _{2b} (msec)	%HbO ₂
1	224	6	223	97*	185	74	202	81
			24	96	138	74	161	80
2	243	12	242	97*	175	75	194	79
			24	93	155	76	180	81
3	214	12	213	97*	154	73	162	75
			24	90	126	72	147	77
4	196	24	194	97*	139	78	122	73
			24	97*	171	77	186	79

* T_{2o} chosen so that %HbO₂ = 97% for blood in aorta for minimum τ₁₈₀ used.

quired at various TEs. These were used to estimate T_{2b} values in the aorta, superior vena cava, and pulmonary trunk. One can observe the blurring in off-resonance regions caused by susceptibility effects (primarily at the chest wall and where pulmonary arteries enter the lungs) when the signal is acquired with spiral gradients of relatively long duration. Nonetheless, the signals in the vessels of interest are well isolated; indeed, virtually no flow-dephasing or wash-in effects are observed in the blood signal, even at the late TEs.

The T_{2b} estimates for this subject and those for several other subjects, determined with the same protocol, are listed in Table 2. Monoexponential decay provides a good fit to the data when estimating the T_{2b} values, although errors are generally greater than those due to random noise alone. Sources of residual error may include dephasing due to complicated flow, the presence of spurious signals, and variations in average R-R interval and breath-hold position between images with different TEs.

These in vivo results reflect, at least qualitatively, the in vitro results. For each subject, venous blood (pulmonary trunk and vena cava) clearly has a shorter T₂ than arterial blood (aorta). In four of the five subjects studied, blood in the pulmonary trunk had a longer T₂ than that in the superior vena cava. One might infer that the %HbO₂ in the pulmonary trunk is greater. Whether this is normally true for healthy subjects is not clear from the medical literature. The range of T_{2b} values is certainly within that measured in vitro. Comparing the T_{2b} values measured with τ₁₈₀ values of 6 and 24 msec in one subject shows a clearly significant decrease in T_{2b} for venous blood at the longer refocusing time, as expected on the basis of the in vitro results. When the difference in τ₁₈₀ values was less (12 vs 24 msec), the results were less conclusive, since the T_{2b} of arterial blood changes almost as much as that of venous blood.

Before one can estimate %HbO₂ from the measured T_{2b} values, the question remains as to the appropriate parametric values to use in Equation (2). Without evidence to the contrary, we assume that the values of K estimated from in vitro data are equally valid for in vivo studies. In choosing T_{2o}, there are several considerations. In healthy subjects at rest, one would expect that %HbO₂ for aortic blood should always be about 97% (26). This implies that T_{2o} should be only slightly greater than

T_{2b} in the aorta. If we fix T_{2o} to the average value obtained from in vitro work, we can expect large errors in estimates of %HbO₂ for arterial blood (eg, estimated %HbO₂ is 83% for a T_{2b} of 194 msec in subject 4, if T_{2o} is 250 msec) or meaningless results if T_{2b} is greater than T_{2o}. If we use measurements of T_{2b} in the aorta to estimate T_{2o}, we are clearly making assumptions about %HbO₂ in the arteries and hence have no predictive power for these vessels. For expediency, we use the latter approach to study %HbO₂ estimation in the venous blood; however, this clearly unsatisfactory state reinforces the earlier conclusion indicating the need for further study of factors affecting T_{2o}. The results are listed in Table 2. The influence of T_{2o} is reduced for the T₂ of venous blood; hence, the difference between estimates of %HbO₂ obtained with the above two approaches for determining T_{2o} is on average about 3%. Except for subject 5, the %HbO₂ estimates would be reduced with a T_{2o} of 250 msec.

The average healthy subject at rest should have an oxygen saturation of about 75% for venous blood (26). The %HbO₂ estimates for the superior vena cava therefore appear reasonable, while those for the pulmonary trunk seem slightly high. In the anecdotal study of τ₁₈₀ effects, predictions of %HbO₂ appear consistent for different refocusing times. These results generally support the applicability of in vitro calibrations to the in vivo measurements. Anecdotal studies of the descending aorta and inferior vena cava in axial images of the abdomen yielded similar results. Still, none of the estimates for deep vessels has been verified by direct, invasive methods of %HbO₂ measurement; therefore, determination of the accuracy of these values remains an important future investigation.

In anecdotal studies of the arm, the relaxation behavior of blood in the deeper arteries and veins paralleled that discussed above. However, for surface veins, estimates of T_{2b} are significantly higher than expected. Because of the accessibility of these vessels to venipuncture, we were able to directly measure %HbO₂ of samples acquired from one such vessel. This measurement confirmed that with the measured T_{2b} values and the mapping function derived earlier (Eq [2]), one would overestimate %HbO₂ significantly in this case. Through a series of experiments, we established that T_{2b} estimates were reduced closer to expected values when the B₀ inhomogeneities due to susceptibility effects

at the skin were eliminated by submerging the arm in water (effects of temperature and different blood flow patterns were factored out through other experiments). We suspect that errors in the quality of signal refocusing in the presence of such inhomogeneities are the source of this effect, prompting further refinement of the train of 180° pulses.

● CONCLUSIONS AND FUTURE WORK

The current work has addressed several challenges in advancing noninvasive estimation of %HbO₂ in vivo by means of relaxation characteristics in MR imaging. The proposed sequence enables accurate measurement of transverse relaxation times in idealized phantom models of vascular blood, even in the presence of steady flow. From in vitro studies with the same imager and effectively the same sequence used for in vivo work, we have quantified the relationship between T_{2b} and %HbO₂. A simplified version of the Luz-Meiboom model of relaxation in the presence of exchange provides a good two-parameter fit to the data. However, more extensive studies are required to adequately examine factors such as individual differences affecting the calibration, particularly those altering the model parameter T_{2o}. For in vivo studies, the measured T_{2b} values for venous and arterial blood and their variation with τ₁₈₀ generally correspond to those expected from the in vitro calibration. Some work must be done to improve the quality of the T_{2b} fits in vivo and to study anomalous T_{2b} values, particularly in surface veins of the arm. Meanwhile, the consistency between %HbO₂ estimates in deep veins (from T_{2b} estimates and application of the in vitro calibration) and their expected physiologic values supports the pursuit of correlative studies with direct measurement of %HbO₂ in veins of interest to examine the accuracy of the proposed method. ●

Acknowledgments: We thank Craig Meyer, MSEE, for supplying the gradient waveforms and reconstruction routines for the spiral readouts and the numerous volunteers for their participation in the experimental studies. We also thank Athos Kasapi, MSEE, for his detailed review of the manuscript.

References

1. Thulborn K, Radda G. Correlation of oxygen consumption with energy metabolism by in vivo NMR. *J Cereb Blood Flow Metab* 1981; 1(suppl 1):S82-S83.
2. Thulborn K, Waterton J, Matthews P, Radda G. Oxygenation dependence of the transverse relaxation time of water protons in whole blood at high field. *Biochim Biophys Acta* 1982; 714:265-270.
3. Gomori J, Grossman R, Yu-Ip C, Asakura T. NMR relaxation times of blood: dependence on field strength, oxidation state, and cell integrity. *J Comput Assist Tomogr* 1987; 11:684-690.
4. Hayman L, Ford J, Taber K, Saleem A, Round M, Bryan R. T₂ effect of hemoglobin concentration: assessment with in vitro MR spectroscopy. *Radiology* 1988; 168:489-491.
5. Terrier F, Lazeyras F, Posse S, et al. Study of acute renal ischemia in the rat using magnetic resonance imaging and spectroscopy. *Magn Reson Med* 1989; 12:114-136.
6. Ogawa S, Lee T, Nayak A, Glynn P. Oxygenation-sensitive contrast in magnetic resonance image of rodent brain at high magnetic fields. *Magn Reson Med* 1990; 14:68-78.
7. Bryant R, Marill K, Blackmore C, Francis C. Magnetic relaxation in blood and blood clots. *Magn Reson Med* 1990; 13:133-144.
8. Matwyoff N, Gasparovic C, Mazurchuk R, Matwyoff G. The line shapes of the water proton resonances of red blood cells containing carbonyl hemoglobin, deoxyhemoglobin, and methemoglobin. *Magn Reson Imaging* 1990; 8:295-301.
9. Luz Z, Meiboom S. Nuclear magnetic resonance study of the protolysis of trimethylammonium ion in aqueous solution: order of the reaction with respect to the solvent. *J Chem Phys* 1963; 39:366-370.
10. Labotka RJ. Measurement of intracellular pH and deoxyhemoglobin concentration in deoxygenated erythrocytes by phosphorus-31 nuclear magnetic resonance. *Biochemistry* 1984; 23:5549-5555.
11. Allerhand A, Gutowsky H. Spin-echo NMR studies of chemical exchange. II. Closed formulas for two sites. *J Chem Phys* 1965; 42:1587-1599.
12. Gillis P, Koenig S. Transverse relaxation of solvent protons induced by magnetized spheres: application to ferritin, erythrocytes, and magnetite. *Magn Reson Med* 1987; 5:323-345.
13. Brooks R, Brunetti A, Alger J, Di Chiro G. On the origin of paramagnetic inhomogeneity effects in blood. *Magn Reson Med* 1989; 12:241-248.
14. Wright G, Nishimura D, Macovski A. Flow-independent MR projection angiography. *Magn Reson Med* 1991; 17:126-140.
15. Levitt M, Freeman R, Frenkiel T. Broadband decoupling in high-resolution nuclear magnetic resonance spectroscopy. *Adv Magn Reson* 1983; 11:47-108.
16. Meyer C, Macovski A, Nishimura D. A comparison of fast spiral sequences for cardiac imaging and angiography (abstr). In: Book of abstracts: Society of Magnetic Resonance in Medicine 1990. Berkeley, Calif: Society of Magnetic Resonance in Medicine, 1990; 403.
17. Pauly J. New approaches to selective excitation for magnetic resonance imaging. Thesis. Stanford University, Stanford, Calif, 1990.
18. Conolly S. Magnetic resonance selective excitation. Thesis, Stanford University, Stanford, Calif, 1989.
19. Mansfield P. Multi-planar image formation using NMR spin echoes. *J Phys C Solid State Phys* 1977; 10:L55-L58.
20. Haase A. Snapshot FLASH MRI: applications to T1, T2, and chemical-shift imaging. *Magn Reson Med* 1990; 13:77-89.
21. MacFall J, Wehrli F, Breger R, Johnson G. Methodology for the measurement and analysis of relaxation times in proton imaging. *Magn Reson Imaging* 1987; 5:209-220.
22. MacFall J, Riederer S, Wang H. An analysis of noise propagation in computed T2, pseudodensity, and synthetic spin-echo images. *Med Phys* 1986; 13:282-292.
23. Majumdar S, Orphanoudakis S, Gmitro A, O'Donnell M, Gore J. Errors in the measurements of T2 using multiple-echo MRI techniques. I. Effects of radiofrequency pulse imperfections. *Magn Reson Med* 1986; 3:397-417.
24. Majumdar S, Orphanoudakis S, Gmitro A, O'Donnell M, Gore J. Errors in the measurements of T2 using multiple-echo MRI techniques. II. Effects of static field inhomogeneity. *Magn Reson Med* 1986; 3:562-574.
25. Bevington P. Data reduction and error analysis for the physical sciences. New York: McGraw-Hill, 1969; 56-64.
26. Ganong W. Review of medical physiology. Los Altos, Calif: Lange Medical, 1981; 520-521.